COMPDYN 2011
3rd ECCOMAS Thematic Conference on
Computational Methods in Structural Dynamics and Earthquake Engineering
M. Papadrakakis, M. Fragiadakis, V. Plevris (eds.)
Corfu, Greece, 25–28 May 2011

NUMERICAL SIMULATION OF BRIDGE PIERS' SEISMIC BEHAVIOR: A BLIND PREDICTION METHODOLOGY

N. Vila – Pouca[1], A. Monteiro[1], A. Arêde[1], P. Delgado[2], R. Delgado[1]

[1] Departamento de Engenharia Civil, Faculdade de Engenharia, Universidade do Porto,
Rua Dr. Roberto Frias, s/n 4200-465 Porto, Portugal
e-mail: nelsonvp@fe.up.pt; abessa@fe.up.pt; aarede@fe.up.pt; rdelgado@fe.up.pt

[2] Escola Superior de Tecnologia e Gestão, Instituto Politécnico de Viana do Castelo.
Av. Atlântico, 4900-348 Viana do Castelo, Portugal
e-mail: pdelgado@estg.ipvc.pt

Keywords: Blind prediction, Seismic Behavior, Numerical Simulation, Bridge Piers, CCBPC 2010.

Abstract. *During mid-2010, the PEER (Pacific Earthquake Engineering Research Center) and NEES (George E. Brown, Jr. Network for Earthquake Engineering Simulation) institutions co-sponsored a shaking table test on a full-scale reinforced concrete bridge pier that was carried out at the UCSD Large High-Performance Outdoor Shake Table. This experimental initiative was encompassed by a worldwide blind prediction contest (Concrete Column Blind Prediction Contest – CCBPC 2010) with over 40 participant teams seeking for the best numerical simulation results. The authors of this paper have participated in that contest and managed to achieve very good results as recognized by an "Award of Excellence" by the contest judges.*

The tested pier was included in a 10.50m high structure, comprising a 5.50m wide footing, a pier body 7.30m high with 1.20m diameter solid circular section. A 250ton reinforced concrete block was placed on the top of the pier in order to drive inertia forces large enough to mobilize the pier capacity, under increasing intensity uniaxial ground motions derived from real earthquake records. The blind numerical analyses were performed knowing only the specimen geometry, reinforcement detailing, material characteristics and the actual ground motions recorded during the testing.

In this context and, in view of the author's participation success, the present paper mainly aims at presenting several aspects of the adopted numerical methodology (and related difficulties) which proved to yield good results, while also providing some insight regarding key problems in numerical simulations of bridge pier seismic behavior. The main numerical and experimental results are compared and a brief discussion is included concerning the reasons for mismatching of some results.

1 INTRODUCTION

Understanding seismic performance of constructions, in general, has been a concern of the scientific community for quite long. That knowledge has met great advances over the last three decades but many problems of earthquake engineering are still difficult to assess in an easy and straightforward way. As an example, most code recommendations are based on reduced scale experimental validation, which for large structures such as bridges, is not easy to accomplish due to a need of considering heterogeneous multi-support excitation [1]. Aiming at providing ever more insight to this particular area, several methodologies and techniques were developed. Such example is the shaking table test, which allows imposing ground motions on structures, attempting to reproduce real earthquake-induced behaviour.

On that particular subject, notable cases can be referred such as the very large E-Defense [2] facility in Japan (some recent works related to it by Yu *et al.* [2010] or Chung *et al.* [2010], ([3,4])), or the NEES [5] equipment sites network of University of Buffalo, SUNY, University of California at San Diego and University of Nevada at Reno (most recent works from NEES@UCSD by Moaveni *et al.* [2010], or NEES@UNR by Johnson *et al.* [2009], ([6,7])). Other smaller scale equipments can be found for example in European facilities such as the Italian EUCENTRE [8], or the French CEA laboratory [9], and even the Portuguese LNEC [10]. Moreover, other relevant testing facilities have been in preparation in the last few years, such as the large shaking table array at Tongji University in Shanghai, China, the Korean laboratory network, and the advanced testing facility currently being developed in the European EFAST program [11].

In the context of scientific testing works carried out resorting to shaking tables, which usually happens with the objective of providing additional information not available from simpler experimental tests, blind numerical prediction initiatives have also been held in the past like SMART 2008 [12], UCSD Englekirk Structural Research Centre's full scale 7 story RC building test [13], or the CAMUS International Benchmark [14,15], the later where some of this paper authors have also participated with great success [16,17,18]. Those simulations are always dependent on deep understanding of the phenomena associated with the seismic behavior of the structures at hand. Besides that, a well-thought methodology needs to be devised in order to adequately address modeling issues without a thorough experimental knowledge.

In light of the documented experience and taking into account the recent results at the Concrete Column Blind Prediction Contest 2010 [19], this paper aims at describing the adopted analysis strategy and, therefore, discussing a number of aspects which are both critical and difficult to evaluate, regarding a given bridge pier seismic behaviour and a correct assessment of its numerical simulation.

2 EXPERIMENTAL CAMPAIGN (CCBPC 2010)

The experimental program associated with the Concrete Column Blind Prediction Contest 2010 initiative was devised by PEER (Pacific Earthquake Engineering Research Center) and NEES (George E. Brown Jr. Network for Earthquake Engineering Simulation) and is briefly described in this chapter. It basically involved of a full-scale reinforced concrete column tested at the UCSD Large High-Performance Outdoor Shake Table [20,21], under uniaxial ground motions with increasing intensity.

2.1 Specimen and material properties

The specimen was a large circular bridge column, bearing a massive concrete block (250 ton) on the top. Figure 1 illustrates its schematic layout and dimensions.

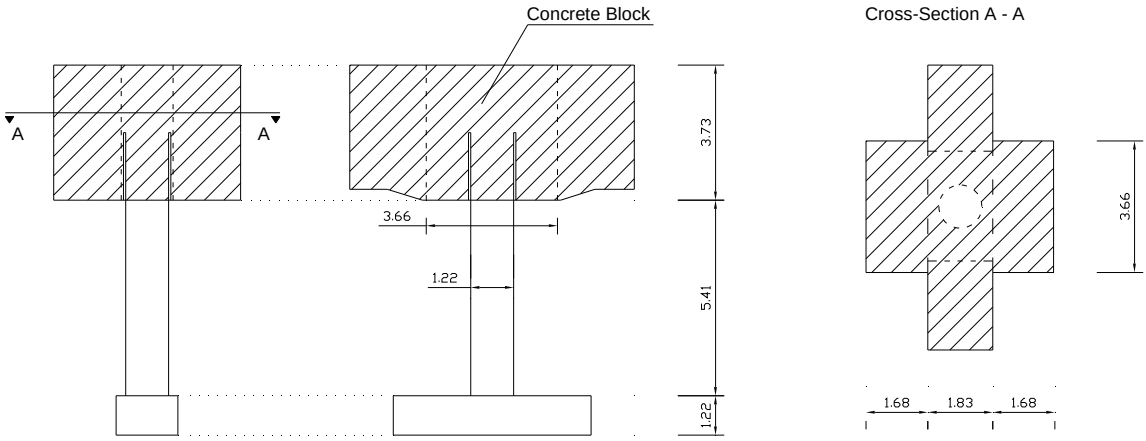

Figure 1 – Column model and dimensions (in meters)

The column was built on the UCSD shaking table, together with two steel-based restraint towers installed around it, in order to prevent excessive (and potentially dangerous) concrete block lateral movements, as depicted by Figure 2 .

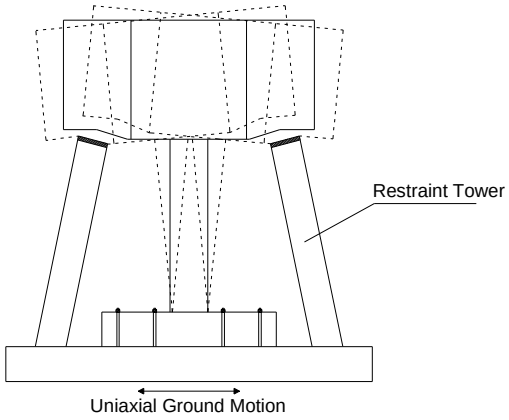

Figure 2 – Restraint towers

The pier's reinforcement steel layout was based on 18 equally spaced No. 11 continuous bars ($\phi \approx 36\,(35.81mm)$). The transverse reinforcement consisted of butt-welded double No. 5 ($\phi \approx 16\,(15.875mm)$) hoops, roughly spaced at 0.15m. The longitudinal bars and circular stirrups development is constant throughout the pier height, both of them penetrating inside the column footing. The properties of the construction materials used in the aforementioned test column were available to all the participant teams and are briefly addressed in the Table 1.

Concrete		Longitudinal Steel		Transverse Steel	
$\sigma_{c\ (21\ days)}$	36.96 MPa	σ_{sy}	518.5 MPa	σ_{sy}	453.7 MPa
$\sigma_{c\ (29\ days)*}$	40.33 MPa	σ_{su}	706.0 Mpa	σ_{su}	592.0 Mpa
$\sigma_{c\ (45\ days)}$	41.85 Mpa				

* - Tests started more than 28 days after concrete casting.

Table 1 – Material Properties

2.2 Instrumentation and Result Demands

The prototype column was densely instrumented in order to obtain good quality results. Specifically, several Linear Voltage Displacement Transducers (LVDTs) were mounted on rods that were rigidly fixed to the concrete column at multiple height levels and accelerations were recorded, using a 16-bit data acquisition system. All the quantities requested in the contest were taken from the resulting data, by direct measurement or implied calculation. Figure 3 describes the aforementioned quantities and the instrumentation layout as used in the tests.

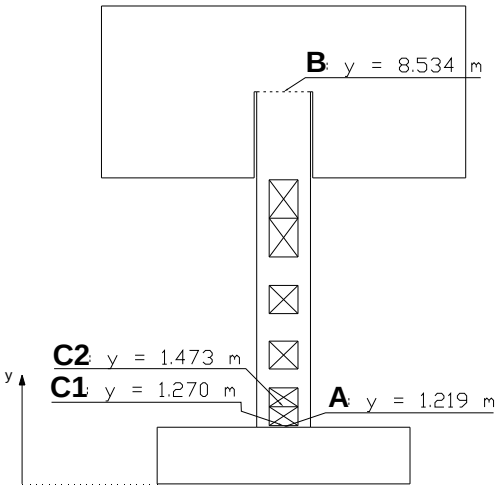

Requested quantities (Maximum values)

1 – Horizontal displacement at level B relative to A
2 – Total horizontal acceleration at level B
3 – Bending Moment at level A (column base)
4 – Shear Force at level A
5 – Average curvature between C1 and C2
6 – Average axial strain between C1 and C2
7 – Residual displacement at level B relative to A
8 – Largest column compressive axial force at level A
9 – Failure Mode

Figure 3 – Instrumentation layout and Contest requested response parameters

2.3 Ground Motions and Test Sequence

Since the experimental programme aimed at assessing the adequacy of design procedures developed by Caltrans to deal with seismic-based structural problems, real earthquake records were used to test the prototype column. Four different acceleration time histories were chosen from Loma Prieta (3 records) and Kobe (1 record) seismic events.

The complete test sequence was performed as described in Table 2, where the really applied seismic events are numbered by even numbers; before each of these six events, a white noise ground motion was applied in order to perform dynamic identification of the system throughout the whole response range.

Event	Ground Motion	Earthquake	Station Name	Scale	Target drift
2	*EQ1*	*Loma Prieta*	*Agnews State Hospital*	1.0 (PGA=4.00 m/s^2)	1%
4	*EQ2*	*Loma Prieta*	*Corralitos*	1.0 (PGA=4.38 m/s^2)	2%
6	*EQ3*	*Loma Prieta*	*LGPC*	1.0 (PGA=4.99 m/s^2)	4%
8	*EQ4 = EQ2*	*Loma Prieta*	*Corralitos*	1.0 (PGA=4.38 m/s^2)	2%
10	*EQ5*	*Kobe*	*Takatori*	0.8 (PGA=5.27 m/s^2)	N/A
12	*EQ6 = EQ3*	*Loma Prieta*	*LGPC*	1.0 (PGA=4.99 m/s^2)	4%

Table 2 – Testing Sequence covering only recorded seismic events

3 MODELLING STRATEGY

This participation in the CCBPC 2010 contest was based in numerical modeling carried out with the Seismostruct analysis software [22]. Since the behavior of the column (due to the uniaxial nature of the table movements) was expected to be dominated by its first vibration mode (because no other significant mass is involved apart from the concrete block), the column was modeled as a simple cantilever structure built upon a sequence of beam elements. Although inelastic force-based elements were used (which helps on reducing the need of a very refined mesh for this type of motion) several finite elements were adopted in order to facilitate the result analysis process, by choosing control sections at appropriate height levels.

The massive concrete block on top of the full-scale column was modeled as a simple lumped mass element at the height level B (y = 8.534m), with corresponding translational mass of 236.15 ton and zero rotational mass moments of inertia.

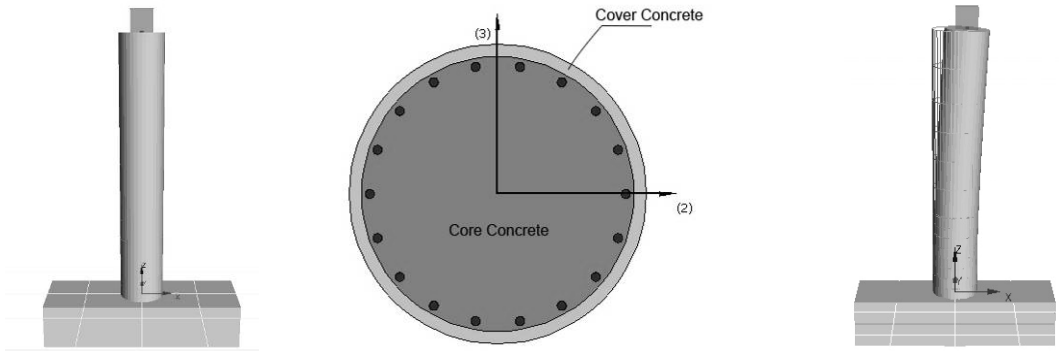

a) Global model illustration b) Cross-section c) First vibration mode (*f=1.46 Hz*) representation

Figure 4 – Numerical finite element model representation

The column cross-section was considered with two distinct zones having different characteristics that were taken into account resorting to the fiber model implemented in Seismostruct. Table 3 includes the parameters used to describe the column behavior of the different types of fibers, while elastic behavior was assumed for the column footing.

A cover band was defined for the peripherical concrete ring, with the remaining cross-section area associated with confined core behavior. Material properties of both zones were defined according to the compressive test results, but an improved scheme was used to simulate the beneficial effect of transverse reinforcement on the core concrete confinement. Thus, Mander's constitutive relations and confinement effects simulation rules [23] were adopted, coupled with cyclic rules proposed by Martinez-Rueda and Elnashai [1997] ([24]), as documented in the adopted software manual.

Cover concrete		Confined Concrete		Longitudinal Steel	
Compressive strength (f_c)	41 MPa	Compressive strength (f_c)	41 MPa	Elastic Modulus (E_s)	200 GPa
Tensile strength (f_t)	3 MPa	Tensile strength (f_t)	3 MPa	Yield Strength (f_y)	520 MPa
Strain at peak stress (ε_c)	0.0028	Strain at peak stress (ε_c)	0.0028	Strain hardening parameter (μ)	0.011
Confinement factor (k_c)	1.0	Confinement factor (k_c)	1.296	R_0 *	20
Unit weight (γ) (kN/m^3)	23.6	Unit weight (γ)	23.6	Unit weight (γ)	77 kN/m^3

Table 3 – Model Properties (*: notation as adopted in [22])

Steel was simulated using the Menegotto-Pinto model [25] implemented in Seismostruct, which also considers isotropic hardening [26]. Default code parameters were used for that purpose, as well as for describing the transition curve.

The above referred modeling aspects are associated with either geometrical or material behavior description issues of an experimental test numerical simulation. However, the most important modeling decisions are strongly related with the seismic loading applied to the structure and to an accurate representation of its effects on the column, because they reflect the dynamic nature of the interaction between the inertia forces (generated by the imposed ground motions) and the non-linear material behavior associated with the accommodation of the developed deformations. Thus, an accurate simulation requires thorough evaluation of the characteristics of both the loading and the structure, in order to understand the influence of some phenomena on the overall column behavior (crack development, stiffness reduction, resonance effects, etc).

The modal analysis of the structural model showed a first vibration mode frequency of 1.46 Hz which is inherently associated with an undeformed state. When drift movements reach a certain level and pier cracks start to develop, the column stiffness drops. This means that the interaction between the loading pattern and the structural response is not constant and can change over time, according to the increasing damage imposed to the column.

The second step in this process consisted on the evaluation of the frequency content of the ground motion signals by means of FFT analyses. Figure 5 displays the FFT amplitude results obtained for each ground motion and a vertical line represents the aforementioned first mode frequency of the structure. Horizontal lines refer to the PGA level of each record adopted.

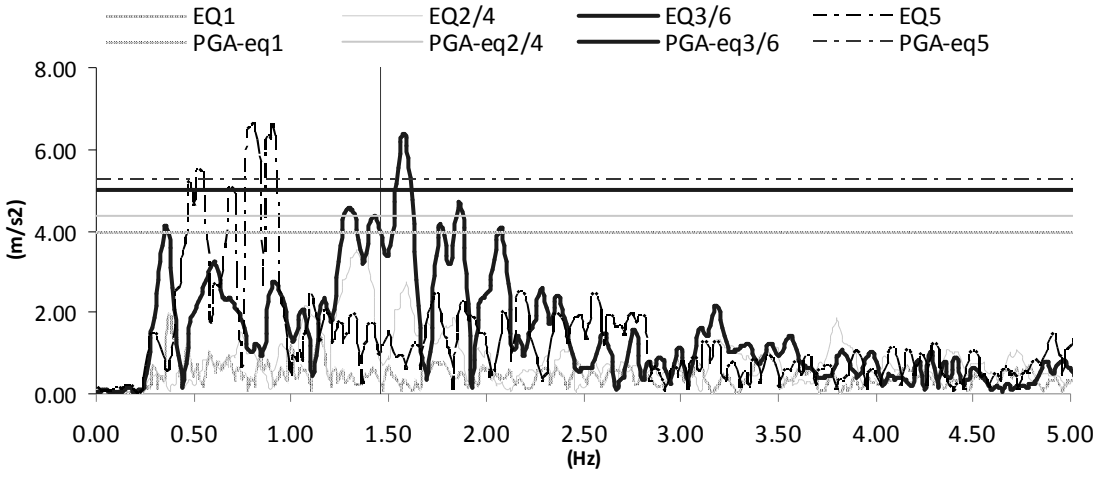

Figure 5 – FFT results for the testing ground motions.

In the previous figure it can be seen that ground motions 2 and 3 have more significant frequency contents around 1.50 Hz (i.e., near the structural frequency). However, once the frequency drops to values slightly smaller than 1.00 Hz, EQ5 can be seen also to have larger significance. In order to better evaluate the inherent consequences, elastic displacement spectra regarding each of the four ground motions were developed for a damping range of 0-2% of the corresponding critical damping. A sound interpretation of such results shown in Figure 6, regarding the experimental sequence which is known beforehand, is very important to understand how the column is likely to perform.

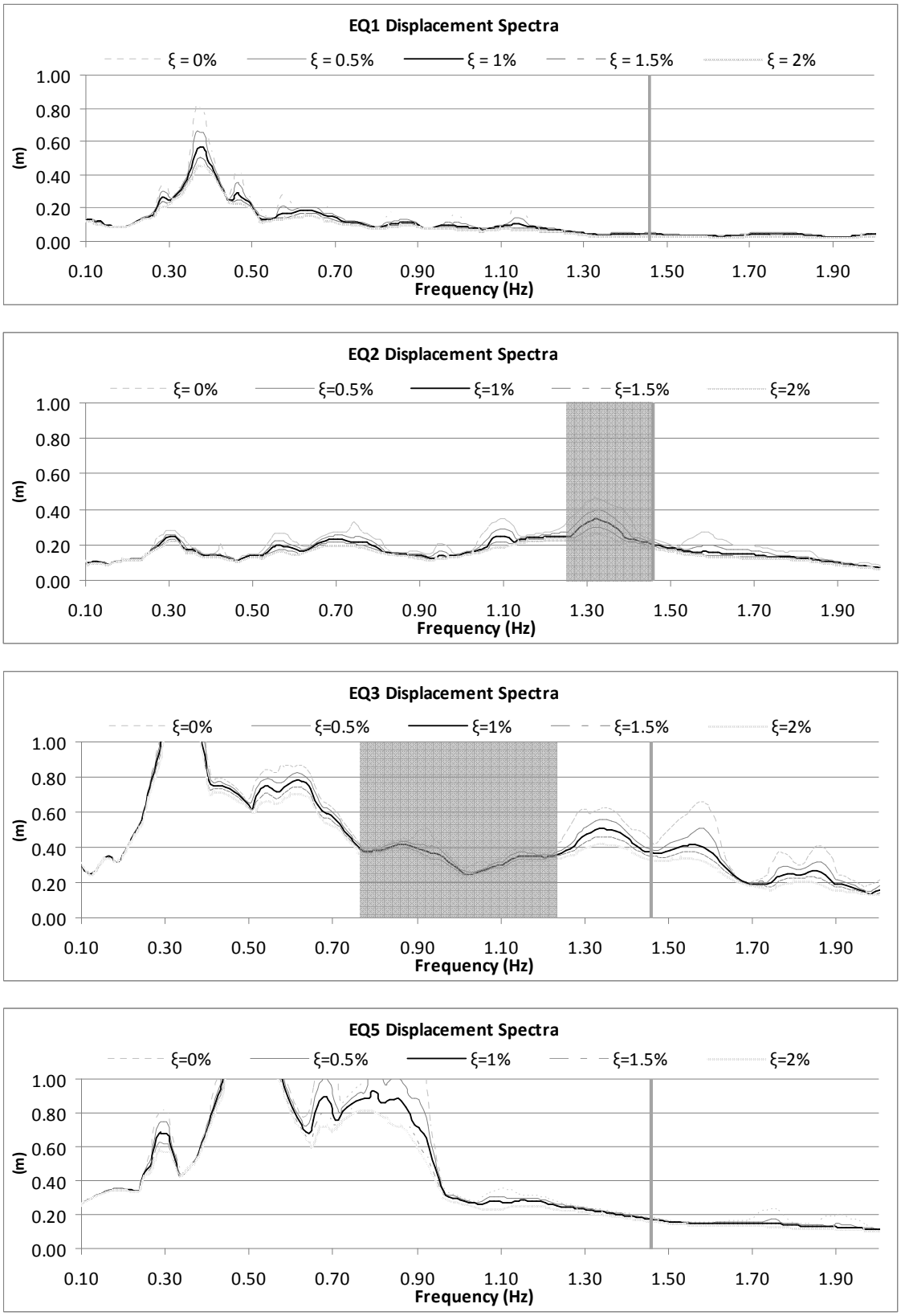

Figure 6 – Elastic displacement spectra due to the imposed ground motions, for several damping ratios

According to Figure 6, the displacement spectra for EQ1 shows low impact for the first vibration mode frequency and also no severe displacement peak in the near range; therefore, it sounds reasonable to assume that the damage imposed to the column during that event was minimal. However, due to low tensile strength of concrete, the column was expected to exhibit cracking on early stages (during EQ2 or even EQ1) leading to stiffness reduction which shifts down the fundamental frequency whose exact range is hard to predict (for that reason, shadow bands are included in the displacement spectra to provide an estimate of the frequency range for the damaged structure). That reduction increases as the concrete cracks develop in size and number, which is consistent with a damage state indicative of moderate non-linear incursion.

As shown in Figure 6, EQ3 ground motion displacement spectra shows relatively uniform values for a wide range of frequencies (within the shadow band) onto which the fundamental frequency is likely to drop. Thus, it is reasonable to assume that important drift values could be reached (say between 200mm and 400mm), regardless of the actually observed column stiffness despite its progressive reduction due to accumulated damage. If the ground motion was shown to be strong enough to induce yielding of the longitudinal rebars, a plastic-hinge mechanism would be due to form, which was further likely to occur because the peak ground acceleration (PGA) was higher for EQ3 than for EQ2.

This reasoning also raises another important point relative to the adopted damping scheme. It is known that viscous damping is especially relevant until the development of a clear hysteretic mechanism, after which the energy dissipation due to hysteretic behavior is much larger than that assumed from viscous damping alone. Therefore, accurate calibration of a numerical model for earthquake simulation requires good viscous damping representation until the plastic-hinge formation and, essentially, good non-linear material behavior description from then onwards. With that in mind, and attempting to reduce the viscous damping impact on the column response after EQ3, the methodology herein adopted was the consideration of a Rayleigh damping matrix matching $\xi = 1\%$ for target frequencies of 1.46 Hz and 0.67 Hz using the tangent stiffness instead of the initial elastic one.

Finally, beyond an effective representation of the interaction between loading, structural properties, viscous damping and hysteretic mechanisms, the time-history analyses of structures subjected to earthquake motions require also an adequate time-step. Thus, in order to correctly represent the loading and to capture its effects on the structure, the time-step of 0.05s was used, which allows vibration components to be adequately described for frequencies of up to 2 Hz.

It should be mentioned that, unlike the experimental activity, no white-noise simulations were made in this work; the ground motions were applied sequentially from EQ1 to EQ6.

4 NUMERICAL SIMULATION RESULTS

The results achieved with the modeling strategy herein presented were generally very good. Although depending on the testing stage, some very significant quantities like top displacement, acceleration or base shear were quite accurately captured, while mainly strains and curvatures exhibited clear deviations from the experimental results. Some of the numerical results are shown in the next paragraphs, generally plotted together with the corresponding experimental results for comparison purposes.

One first issue to be addressed relates to residual displacements that can reach important figures but may not be easily captured in numerical analyses. In order to identify the performance of numerical simulations on this particular issue, shows the complete sequential re-

sponse of the numerical model in terms of top displacement; horizontal lines corresponding to the numerical and experimental residual displacements are also included in order to compare permanent deformation levels captured with this modeling strategy and those recorded in the experimental test.

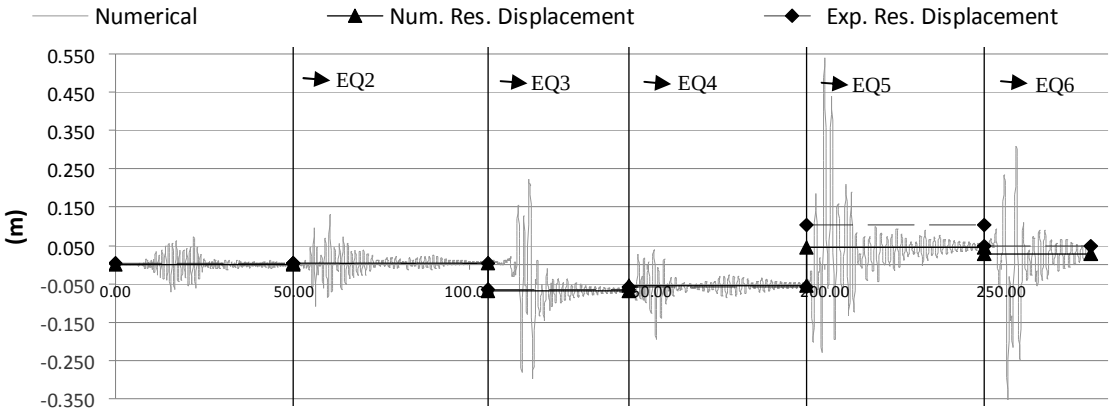

Figure 7 – Complete series of numerical top displacement time-histories with residual displacements (numerical and experimental).

Results show that residual deformations were quite accurately captured except for EQ5, where the difference was larger. It indicates that the overall column stiffness level and material properties were adequately simulated, since each ground motion was able to reproduce the same deformation levels on both the experiment and its numerical model. Non-linear progression might have been similar, although this argument needs further support in view of the difference shown for EQ5 where plastic hinging was due to be established.

A more in-depth, motion by motion, analysis can provide additional information regarding this modeling strategy's adequacy to the blind prediction problem.

Taking for example the horizontal acceleration time histories represented in -a) for the first stage (EQ1), both experimental and numerical curves seem to be in good agreement, with slight numerical overestimation of peak values, until approximately 23s. From then on, i.e., after the peak displacement values, the experimental period elongation was more evidenced than in the numerical response, which might have been due to more damage in the real test. This effect contributes, not only for the period elongation, but also to the increase of damping which is reflected in lower experimental displacements (than the numerical ones) around the 30s time instant.

Similar conclusions are drawn for the corresponding displacement time histories -b) and it is worth mentioning that, by the end of this test (EQ1) when displacements become smaller, the numerical response shows lower values than the experimental one. This modification of the relative magnitude of experimental and numerical response might be explained by the difficulties on achieving a robust simulation of damping that is able to follow adequately the response both in the large and small amplitude cycles.

This issue was also observed for other earthquake motions but, unlike EQ1 where the post-peak differences were mild, larger discrepancies were observed between numerical and experimental curves for the other earthquakes, on the post-peak range, as shown for instance in the top horizontal acceleration time-history for EQ2 (see Figure 9).

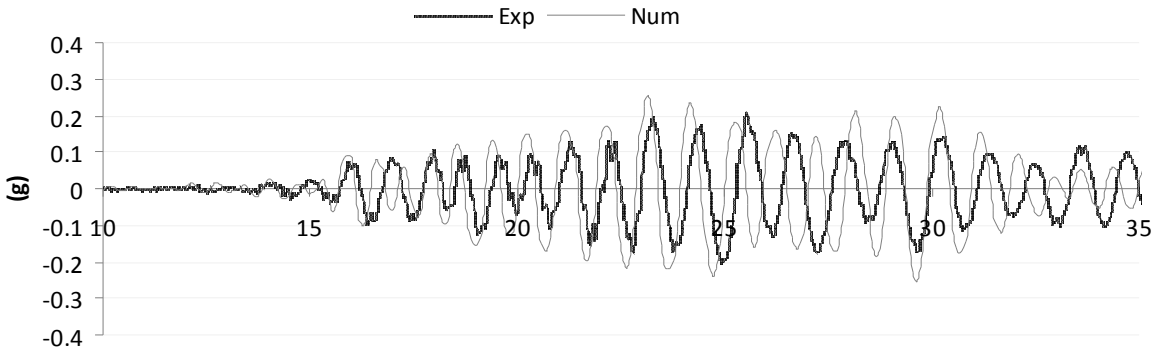

a)

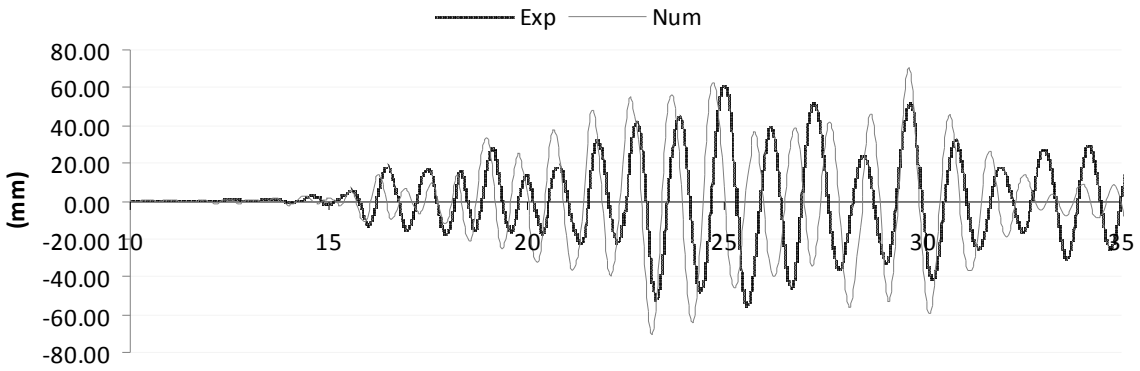

b)

Figure 8 – Numerical vs. Experimental time histories of horizontal a) acceleration and b) displacements (EQ1).

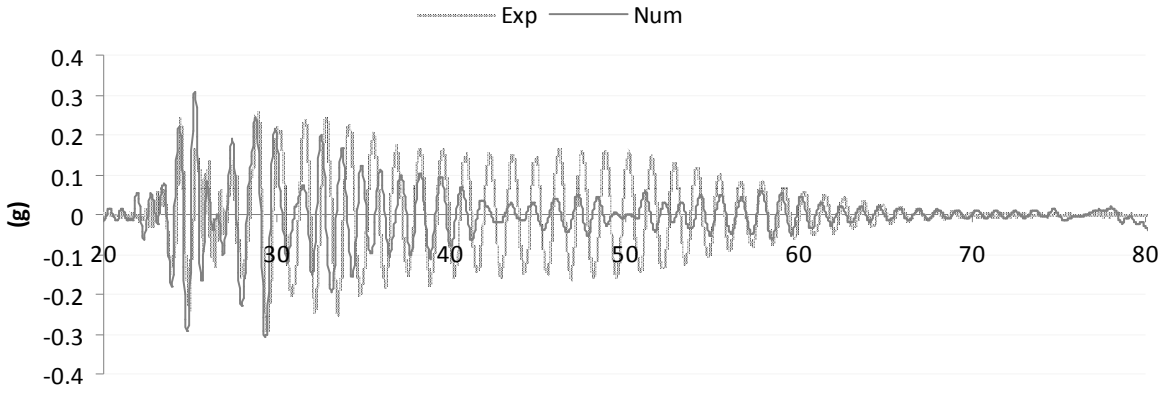

Figure 9 – Numerical vs. Experimental horizontal acceleration time-history (EQ2).

In contrast however, EQ3 showed remarkable results for a blind prediction, with almost all parameters simulated with quite good accuracy (as globally depicted in Figure 10).

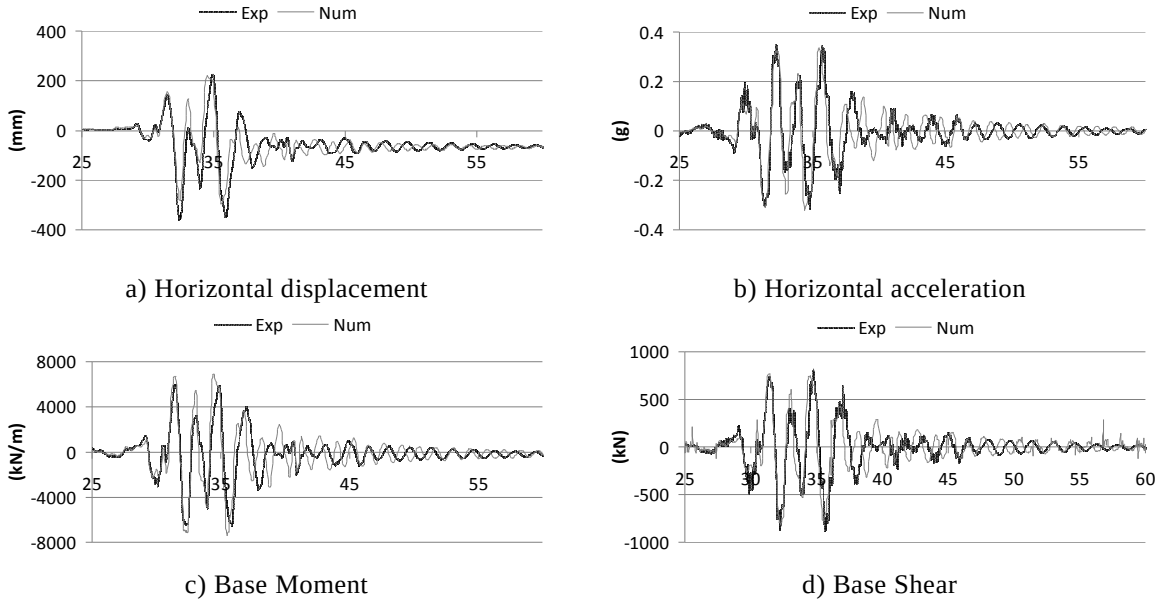

a) Horizontal displacement

b) Horizontal acceleration

c) Base Moment

d) Base Shear

Figure 10 – Numerical vs. Experimental horizontal results (EQ3).

This was especially important because EQ3 was the first ground motion to clearly push the column into plastic behavior of the longitudinal reinforcement as it was predicted (see Figure 11, where the complete time history of longitudinal reinforcement stress is compared against the yielding threshold). Therefore, the plastic hinge formation was adequately captured by the numerical model.

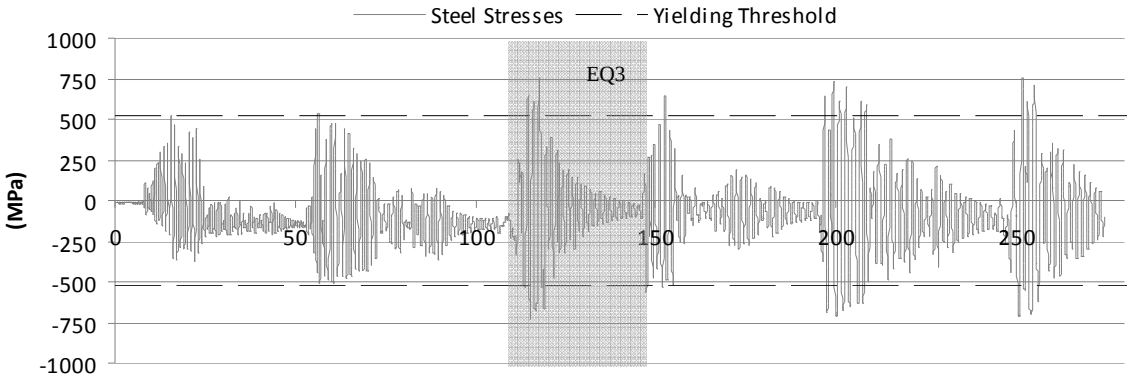

Figure 11 – Complete longitudinal reinforcement stress time-history.

Since the numerical simulation was so similar to the experimental results for this specific ground motion, it follows that the adopted damping was probably accurate enough to provide a good balance between viscous damping during EQ1 and EQ2 (especially concerning peak response values), while making sure the plastic hinge contribution was the main dissipation mechanism once it formed.

It is noteworthy that, for plastic behavior clearly installed (as for EQ3), the influence of viscous damping, adopted to simulate (essentially) the cracking stage preceding the yielding

threshold, becomes less important in global response, particularly in what concerns peak values.

This is further confirmed with the response simulation for EQ5earthquake, which has exhibited quite satisfactory agreement between numerical and experimental results (Figure 12) for the same parameters as for EQ3, notwithstanding the fact (already stated before) that deformation measures (axial strain and curvature) were not accurately simulated in the post-peak behavior.

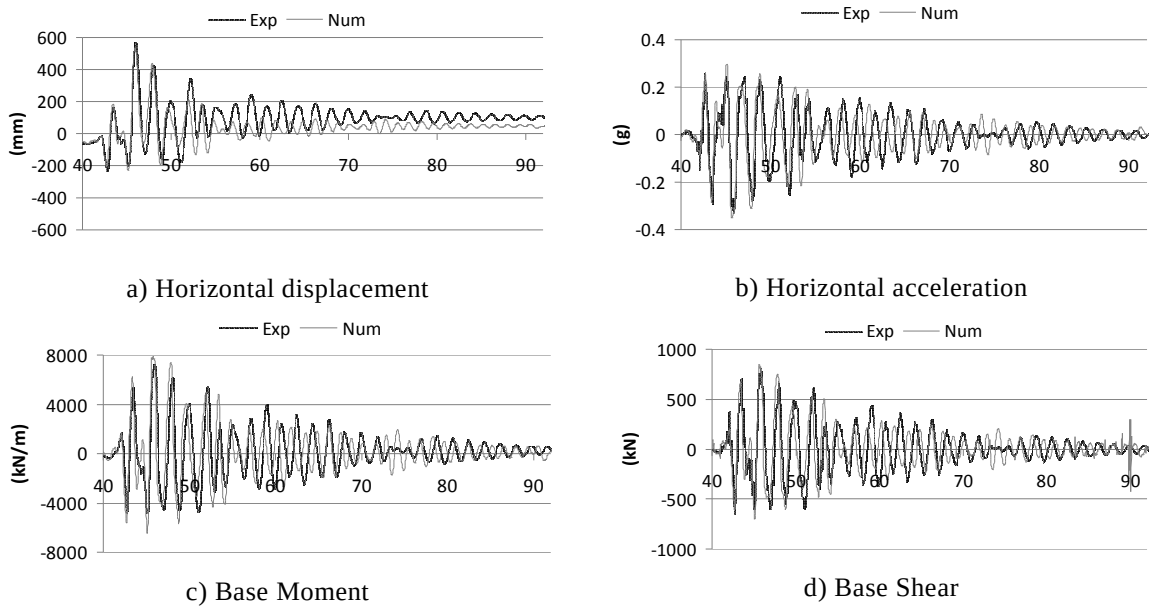

a) Horizontal displacement

b) Horizontal acceleration

c) Base Moment

d) Base Shear

Figure 12 – Numerical vs. Experimental horizontal results (EQ5).

From the above described, an overall observation allows confirming that very satisfactory results were obtained. Differences focused mainly on the column post-peak behavior for each time-history, encompassed by slight out-of-phase response records due to difficulties on simulating accurately the cracking (thus affecting the fundamental period of vibration). Inaccurate residual deformations in the numerical modeling were also identified, although mainly for the EQ5 motion.

5 CONCLUSIONS

This paper described the work carried out by the authors in the framework of their participation in the Concrete Column Blind Prediction Contest 2010 sponsored by PEER and NEES. The blind numerical analyses were presented, preceded by a brief description of the strategy upon which the modeling decisions were made. That was based in simple procedures to evaluate the impact of the seismic loading (such as FFT analyses) and a refined characterization of the structural model using well proven constitutive relations, wherein confinement effects were also considered. The interaction between the seismic loading and the resulting structural degradation was addressed as being of key importance. The former directly increases the latter which, in turn, influences the intensity of the structural response. An adequate representation of the energy dissipation mechanisms was devised for this case, namely by adopting a suitable compromise between structural viscous damping and non-linear material behavior. As expected, the influence of the former was found of greater importance up to the plastic-hinge formation point.

The six ground motions were applied to the numerical model and the results obtained were compared against the test recorded values. The scenario was globally very good. Peak values were simulated with little difference relative to their experimental counterparts (like horizontal displacement and acceleration, base shear, etc) and overall time-history responses exhibited similar behavior. The main negative aspects of this modeling strategy consisted on the difficulties to reproduce adequately the strain and curvature values (probably related to the way they are recorded in the test and read in the numerical simulation), as well as mismatching the post-peak vibration period and the residual deformation from ground motion EQ5. Nonetheless, the plastic-hinge formation was quite accurately predicted.

However, perhaps the most important issue of this work was the development of a good perception of the evolution of the column non-linear response in order to enable and control the model for addressing the involved and relevant phenomena. Without a clear understanding of such phenomena, as well as the overall reinforced concrete cyclic behavior, simulation would be hardly feasible because any modeling could have many shortcomings and lead to considerable differences. Therefore, successful results within a blind prediction process reflect, not only the quality of the tools used in the work, but also the analysts ability to predict the key issues of the structural response.

REFERENCES

[1] Marazzi, F., Politopoulos, I. and Pavese, A., An overview of seismic testing needs in Europe: towards a new advanced experimental facility. *Bulletin of Earthquake Engineering* DOI 10.1007/s10518-010-9212-8, 2010.

[2] http://www.bosai.go.jp/hyogo/ehyogo/

[3] Yu, Y., Tsai, K., Weng, Y., Lin, B. and Lin, J., Analytical studies of a full-scale steel building shaken to collapse. *Engineering Structures*, **32**, 3418-3430, 2010.

[4] Chung, Y., Nagae, T., Hitaka, T. and Nakashima, M., Seismic Resistance Capacity of High-Rise Buildings Subjected to Long-Period Ground Motions: E-Defense Shaking Table Test. *Journal of Structural Engineering*, ASCE, **136** (6), 637-644, 2010.

[5] http://nees.org/sites-mainpage/shaketablelabs/

[6] Moaveni, B., He, X., Conte, J. and Restrepo, J., Damage identification study of a seven-story full-scale building slice tested on the UCSD-NEES shake table. *Structural Safety*, **32**, 347-356, 2010.

[7] Johnson, N., Saiidi, M. and Sanders, D., Nonlinear Earthquake Response Modeling of a Large-Scale Two-Span Concrete Bridge. *Journal of Bridge Engineering*, ASCE, **14** (6), 460-471, 2009.

[8] http://www.series.upatras.gr/EUCENTRE

[9] http://www-tamaris.cea.fr/html/en/tests/azalee.php

[10] http://www.series.upatras.gr/LNEC

[11] Marazzi, F. and Molina, F., 1st EFAST workshop—challenges, needs and open questions. *EUR 23822 EN*. Luxembourg: Publications Office of the European Union. JRC5 51632, 2009.

[12] Varpasuo, P. and Kâhkönen, J., Blind prediction of smart 2008 seismic structural response test results. *Proceedings of the International Conference on Nuclear Engineering, ICONE*, **4**, 131-137, 2008.

[13] Kelly, T., A blind prediction test of nonlinear analysis procedures for reinforced concrete shear walls. *Bulletin of the New Zealand Society for Earthquake Engineering*, **40** (3), 142-159, 2007.

[14] CIB-RI, CAMUS International Benchmark - Report I, Mock-Up and Loading Characteristics. Specifications for the Participants Report. *Report SEMT/EMSI/RT/98-066A*, CEA, France, 1998.

[15] CIB-RI, CAMUS International Benchmark - Experimental Results. Synthesis of the Participants Reports, *Report SEMT/EMSI/RT/98-067A*, CEA, France, 1998.

[16] Faria, R., Vila-Pouca, N. and Delgado, R., Seismic Behaviour of a RC Wall: Numerical Simulation and Experimental Validation. *Proceedings of the IV Congreso de Métodos Numéricos en Ingeniería* (CD-ROM), Seville, Spain, 1999.

[17] Vila-Pouca, N., Faria, R. and Delgado, R. Prediction Analysis of a Reduced Scale Wall Building. *Relatório sobre a Participação da FEUP no "CAMUS 1 International Benchmark"*, Faculdade de Engenharia da Universidade do Porto, Porto, Portugal, 1998.

[18] Vila-Pouca, N., Faria, R. and Delgado, R., Numerical Simulation of the Seismic Behaviour of a Reduced Scale RC Wall Building. *Relatório sobre a Participação da FEUP no "CAMUS 3 International Benchmark"*, Faculdade de Engenharia da Universidade do Porto, Porto, Portugal, 2000.

[19] http://nisee2.berkeley.edu/peer/prediction_contest/

[20] Restrepo, J., Conte, J., Luco, J., Seible, F. and Van den Einde, L., The NEES@UCSD large high performance outdoor shake table. *Geotechnical Special Publication*, (130-142), 931-946, 2005.

[21] Ozcelik, O., Luco, J., Conte, J., Trombetti, T. and Restrepo, J., Experimental characterization, modeling and identification of the NEES-UCSD shake table mechanical system. *Earthquake Engineering and Structural Dynamics*, **37**, 243-264, 2008.

[22] www.seismosoft.com

[23] Mander, J., Priestley, M. and Park, R., Theoretical Stress-Strain Model for Confined Concrete. *Journal of Structural Engineering*, ASCE, **114** (8), 1804-1826, 1988.

[24] Martinez-Rueda, J. and Elnashai, A., Confined concrete model under cyclic load. *Materials and Structures*, **30** (197), 139-147, 1997.

[25] Menegotto, M. and Pinto, P., Method of analysis for cyclically loaded reinforced concrete plane frames including changes in geometry and non-elastic behaviour of elements under combined normal force and bending. *IABSE Symposium on Resistance and Ultimate Deformation of Structures Acted on by Well-Defined Repeated Loads*, Final Report, Lisbon, 1973.

[26] Filippou, F., Popov, E. and Bertero, V., Modelling of R/C joints under cyclic excitations. *Journal of Structural Engineering*, ASCE, **109** (11), 2666-2684, 1983.